Quantitative MR Imaging Study of Intravitreal Sustained Release of VEGF in Rabbits

Nadir Alikacem,[1] *Toyohisa Yoshizawa,*[1,2] *Kevin D. Nelson,*[3] *and Charles A. Wilson*[1]

Purpose. To determine whether sustained elevation of vascular endothelial growth factor (VEGF) in the vitreous cavity causes retinal hyperpermeability [blood–retinal barrier (BRB) breakdown] before the development of retinal neovascularization (NV) and to document the kinetics of the integrity of BRB breakdown versus time.

Methods. Poly(L-lactide-*co*-glycolide)-based devices loaded with VEGF were implanted intravitreally in rabbit eyes. Contrast-enhanced magnetic resonance imaging (MRI) methods were used to identify and quantitate the retinal permeability at various time points after implantation. This was done with the newly developed MR tracer AngioMARK (Epix Medical, Boston, MA). After the MRI measurements, fundus photography and fluorescein angiography (FA) also were performed on the same set of animals.

Results. At 3 days after implantation, the MR images showed a significant retinal leakage into the vitreous cavity (BRB breakdown) of the VEGF-implanted eyes. To quantitate this leakage, the permeability surface area product (PS) was measured. At 3 days, the mean PS product was $1.25 \pm 0.25 \times 10^{-5}$ cm^3/min. Based on the VEGF in vitro release study, this 3-day BRB breakdown corresponded to a total sustained release of 7.42 ± 0.54 μg/ml of VEGF. The fundus and FA photographs of these VEGF-implanted eyes taken at 4 days after implantation also showed a considerable level of retinal vascular dilation and tortuosity. By 12 days after implantation, the mean PS product decreased to $5.83 \pm 1.38 \times 10^{-6}$ cm^3/min. However, the retinal NV was observed only after the second week after implantation. By this time, a total of 10.70 ± 0.92 μg/ml of VEGF was released in a sustained fashion. Also, after the retinal NV development, retinal detachment also was observed. The control eyes, however, which were implanted with blank devices, remained unchanged and normal during the entire course of this study (PS = $5.57 \pm 0.66 \times 10^{-7}$ cm^3/min).

Conclusions. The findings indicate that sustained delivery of elevated amounts of VEGF in the vitreous cavity induces a BRB breakdown even earlier than 3 days after implantation. This was achieved after a total sustained release of 7.42 ± 0.54 μg/ml of VEGF. This retinal leakage regressed by more than half by the time the retinal NV developed. Furthermore, a retinal detachment occurred after this retinal NV. These results are similar to proliferative diabetic retinopathy (PDR). The sustained elevation of VEGF in the vitreous cavity of rabbit eyes is potentially a good model to test VEGF antagonists to treat or prevent PDR in humans. The quantifiable change of BRB breakdown by the contrast-enhanced MRI method is ideal to assess the therapeutic intervention in vivo without killing the animal and may prove to be clinically useful in humans. (*Invest Ophthalmol Vis Sci.* 2000;41:1561–1569)

Vascular endothelial growth factor (VEGF) is a very potent inducer of angiogenesis,[1] is known to induce hyperpermeability of microvessels,[2,3] and is also a major factor in the pathogenesis of ischemic retinopathies such as diabetic retinopathy (DR),[4] which is a leading cause of new blindness in the western world. VEGF is upregulated by tissue ischemia/hypoxia, which results from retinal vascular obstruction in the relatively late stages of DR.[5] Elevation of VEGF in the retina and the vitreous were reported in both humans[4] and animal models[6] with ischemic retinopathies. Furthermore, VEGF is suggested to play a significant role even in nonproliferative DR.[1,7,8] It was reported that the continuous hyperglycemic environment in diabetes and the continuous low perfusion of peripheral retinal tissue also might contribute to the upregulation of VEGF.[1,9] As a consequence, VEGF contributes to the changes in retinal hemodynamics and morphology observed in early DR.[7]

VEGF is secreted by several ocular cell types, including endothelial cells, pericytes, ganglion cells, Müller cells, and photoreceptor cells.[5,6,10–12] Retinal endothelial cells have a high affinity for VEGF. They not only have both the mechanism to secrete VEGF, but also a greater number of VEGF receptors than found on other endothelial cells.[13] Sustained delivery of elevated amounts of VEGF in the vitreous cavity led to the

From the [1]Department of Ophthalmology, University of Texas Southwestern Medical Center at Dallas, Texas; [3]Department of Biomedical Engineering, University of Texas Arlington, Texas; and [2]Department of Ophthalmology, Niigata University, School of Medicine, Niigata, Japan.

Supported by Research to Prevent Blindness.

Submitted for publication July 8, 1999; revised December 7, 1999; accepted December 20, 1999.

Commercial relationships policy: N.

Corresponding author: Nadir Alikacem, Department of Ophthalmology, UT Southwestern Medical Center at Dallas, 5323 Harry Hines Boulevard, Dallas, TX 75235-8592. nalica@mednet.swmed.edu

development of retinal neovascularization (NV) in the rabbit animal model.[14] This recent demonstration has prompted investigators to use this potential model for testing VEGF antagonists for inhibiting retinal NV and retinopathies in humans. It is not clear, however, if in the early stages of sustained release of VEGF in the vitreous cavity, VEGF causes breakdown of the blood–retinal barrier (BRB). The goals of this study were (1) to determine whether VEGF causes breakdown of the BRB before the development of retinal NV, (2) how soon after implantation BRB breakdown occurs, and (3) to document the integrity of this BRB breakdown versus time. To carry out this study, we implanted poly(L-lactide-*co*-glycolide) copolymer (PLGA)-based devices loaded with VEGF in the vitreous cavity of rabbit eyes. The BRB breakdown was investigated by contrast-enhanced magnetic resonance imaging (CE-MRI) methods.

MR contrast agents, such as gadolinium diethylenetriaminepentaacetic (Gd-DTPA), have been widely used to investigate abnormal leakage in the blood–brain barrier,[15,16] and retinal lesions.[17,18] The alterations in the leakage are used to determine the history of the diseases. The combination of a long T_1 of the vitreous and short echo time (TE) and repetition time (TR) used in the spin-echo pulse sequence allows the acquisition of T_1-weighted MR images (T_1 is the longitudinal MR relaxation time). The signal intensity enhancement in these images is mainly caused by the T_1 relaxation effect of local contrast agent concentration. The presence of the contrast agent facilitates the relaxation of the surrounding vitreous water protons, leading to shorter relaxation times. This allows good correlation between the relative signal intensity and local contrast agent concentration. Unlike other anatomic sites with heterogeneous tissues and different T_1s, the homogeneity of the vitreous allows a more accurate assessment of local contrast agent concentration because of the uniform relationship between the contrast agent and the vitreous protons. Consequently, a quantitative measure of the entry of the contrast agent into the vitreous cavity can be obtained from the contrast enhanced MR signal intensities.[19] This leakage into the vitreous cavity indicates the retinal hyperpermeability (breakdown of the BRB). This study is done with AngioMARK MR contrast agent (Epix Medical, Boston, MA). Its relaxivity in both human and rabbit plasma ($R = 53.5 \pm 3.8$ l and 32.5 ± 2.3 l/mmol/sec, respectively) is at least eight times higher than that of GdDTPA-based contrast agent,[20] which is 4.7 ± 0.3 l/mmol/sec. Furthermore, AngioMARK has a much more prolonged plasma half-life. These properties, in addition to being highly protein bound, made AngioMARK ideal for the present study. Increased relaxivity and plasma half-life causes an increase in the MR signal intensity and therefore a higher sensitivity in detecting retinal leakage into the vitreous cavity.

Materials and Methods

Polymer Devices

Degradable poly(L-lactide-*co*-glycolide) (PLGA) copolymers of composition 50 mol % of L-lactide and 50 mol % glycolide (Sigma-Aldrich, St. Louis, MO) were used to fabricate the VEGF sustained delivery devices in the form of a bolt with an overall length of 3.5 mm with a 1-mm-diameter shaft. The head of the device was approximately 2 mm in diameter and 1 mm in length. The polymeric devices were prepared by dissolving 0.31 g of PLGA in 1.2 ml of methylene chloride (Sigma-Aldrich). The VEGF solution was prepared by dissolving 230 μg of VEGF in 1 ml of saline solution that contained 27.9 mg of bovine serum albumin (BSA; Sigma-Aldrich), and 61 mg of poly(vinyl alcohol) (PVA; Sigma-Aldrich). This VEGF solution was then added to the PLGA solution, emulsified using a vortex genie (Fisher Scientific, Pittsburgh, PA) for 2 minutes, and immediately dipped in dry ice-acetone solution for a quick freeze. The frozen emulsion was then lyophilized for 24 hours to obtain a spongelike polymer structure. This was pressed into plugs weighing 20 mg containing 14.9 μg VEGF and 1.8 mg BSA. Identical plugs also were made without the VEGF to serve as control plugs.

In Vitro Release of VEGF

The VEGF-loaded plug was placed into 0.5 ml of 0.9% sodium chloride saline in a closed vial and immersed in a water bath at 37°C. At predetermined intervals, the released medium was removed and replaced with the same quantity of fresh medium. The amount of VEGF released was measured using a commercially available VEGF sandwich enzyme-linked immunosorbent assay (ELISA) kit (Chemicon International, Temecula, CA). The optical density of each well was measured by a plate reader using a 490-nm filter, and the VEGF content was estimated from the standard curve. The range of detection of this ELISA kit is 20 to 2500 pg/ml.

Animals and Anesthesia

Five male Dutch Belted rabbits weighing approximately 2.5 kg were used in these experiments. The animals were treated in accordance with the ARVO Statement of the Use of Animals in Ophthalmic and Vision Research, the NIH Guide for the Care and Use of Laboratory Animals, and our institutional guidelines on the use of animals in research. Anesthesia was introduced by intramuscular (IM) injection of ketamine HCl (35 mg/kg) and xylazine HCl (5 mg/kg). During the MRI procedures (as described below), anesthesia was maintained with continuous intravenous (IV) infusion of ketamine HCl (20–40 mg/kg/h) and xylazine HCl (2–4 mg/kg/h) via an auricular venous catheter (Becton Dickinson, Sandy, UT).

The pupils were dilated before surgery with 2.5% neosynephrine and 1% tropicamide eye drops. A 9-0 monofilament, Prolene suture (ETHICON, Somerville, NJ) was tied securely around the shaft of the implant. The conjunctiva was reflected with scissors and blunt dissection exposing bare sclera on the superior side of the globe and on the nasal side of the superior rectus muscle. A circumferential incision was created with a myringotomy blade approximately 3 mm in length, 4.0 mm from the limbus. Any bleeding that was encountered generally remained external to the eye and was allowed to clot spontaneously. Any prolapsed vitreous and clot was then cleanly removed using scissors. The implant was inserted into the vitreous space and secured to the wound edges using the original 9-0 Prolene suture. The suture was then used to close the wound in a continuous fashion. The conjunctiva was reapproximated with a single 8-0 vicryl suture (ETHICON). The eye was then examined with a flat contact lens to determine whether the implant was in a satisfactory location. A small amount of vitreous hemorrhage was present in most eyes. However, animals that showed retinal detachment were excluded. Tobrex ointment (Alcon Laboratories) was given immediately after the surgery and twice daily for 3 days.

Magnetic Resonance Imaging

The animals were examined using MRI on postimplantation days 3, 12, 19, and 27. The MRI study was performed on a Philips Gyroscan ASCS-NT 1.5 T clinical scanner (Philips, Eindhoven, The Netherlands) using an 8-cm surface coil. Before the MR imaging experiments, each animal was anesthetized as described above and then was gently placed in a Plexiglas cradle in the supine position. This cradle was then put on the MRI examination table. The core body temperature was maintained within the normal range using a circulating blanket connected to a constant temperature bath. Axial T_1-weighted images (spin-echo pulse sequence, TR/TE = 450/18 msec, NEX = 3, a matrix of 256 × 256, and FOV of 8 cm) with a slice thickness of 2.5 mm were obtained through the geometric center of both eye globes of the animal. These slices were oriented perpendicular to the long axis of the vascularized medullary ray. Each image required 3 minutes and 52 seconds to acquire. A control image is acquired first, followed by a bolus IV injection of the newly developed MR contrast agent AngioMARK (0.1 mmol/kg; Epix Medical).[20,21] Four sequential postinjection images were then acquired.

MR Image Analysis

The MR image analysis was carried out in the same fashion as previously reported.[17–19,22–24] These images were analyzed using the NIH program Image for PC (Scion Corporation, Frederick, MD). In-house developed subroutines were used to calculate the permeability surface area product (PS; in cm^3/min).[17–19,22–24] The analysis consisted of defining a region-of-interest (ROI) within the vitreous that contains all visible signal enhancement on the final image, obtaining a mean signal intensity over that ROI and applying that same ROI to the other images in the set. An external vial (1.3-cm inner diameter) containing Gd-DTPA–doped water was included in each image and provided the spatial calibration (number of pixels/cm) needed for determining the area of the ROI. The PS of each lesion was calculated for all postinjection images. The postinjection times are defined as the time between the center of AngioMARK injection and the center of image acquisition, approximately 2, 7, 12, and 16 minutes for the 1st, 2nd, 3rd, and 4th postinjection images, respectively.

Fluorescein Angiography

The fluorescein angiography (FA) techniques are noninvasive methods, and therefore they are an ideal complement to the MRI techniques that we used in this study. FA was performed either the day before or after the MRI measurements on both eyes of the same set of animals. After administration of 10% sodium fluorescein (0.1 ml/kg; Alcon Laboratories) via the marginal ear vein, fluorescein angiography was performed using a Topcon TRC-50X fundus camera (Topcon, East Paramus, NJ).

Results

VEGF In Vitro Release Study

The cumulative release of VEGF from the plug is plotted in Figure 1. The results show that approximately 80% of VEGF in the plug was released throughout a 3-week period. During this period, the plug had a biphasic release pattern: an initial burst during the 1st week and a linear release thereafter. The amount of VEGF released after 24 hours and 3 days of incubation was 6.28 ± 0.36 and 7.42 ± 0.54 μg/ml (mean ± SE), respectively.

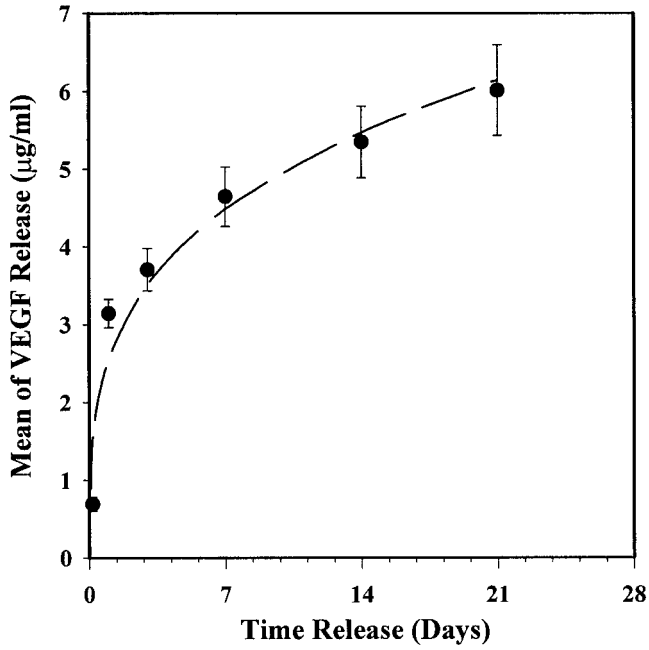

Figure 1. Cumulative release of VEGF from the PLGA delivery device in 0.5 ml of 0.9% sodium chloride saline at 37°C. These data are fitted to a power function of time t, $f(t) = kt^n$, using a nonlinear square fit algorithm[32]; $k = 2.57 \pm 0.031$ and $n = 0.29 \pm 0.05$. This suggests that the VEGF release was governed by diffusion-like process.

CE-MRI Qualitative Description

PLGA-based devices loaded with 14.9 μg VEGF were implanted into the vitreous of the left eye of five rabbits. Identical blank devices, that is, without VEGF, were implanted into the vitreous of the right eye of the same rabbits. Both eyes of the same animal were used to determine the effects induced by the surgical procedure, the presence of the PLGA plug, the release of BSA and PVA, and the acidic environment produced by the degradation of the polymer. In this way, it was possible to isolate the effect caused by the presence of VEGF in the eye.

Figure 2A is representative of MR images that were obtained through the geometric center of both eye globes of rabbits before injecting the contrast agent AngioMARK. Figures 2B through 2E show the same image 2, 6.7, 10.7, and 15.2 minutes after injecting the contrast agent, respectively. The images of Figure 2 were acquired 3 days after implantation. The signal intensity enhancement in these images is mainly caused by the T_1 relaxation effect of local contrast agent concentration. The contribution of T_2 relaxation by this contrast agent is negligible. Consequently, Figures 2B through 2E show the entry of the contrast agent into the vitreous space of the left eye, as indicated by the intensity change on the T_1-weighted images (indicated by the arrows), whereas the control eye remained unchanged. This entry of the contrast agent into the vitreous space indicates the breakdown of the BRB of the left eye at 3 days after implantation. A similar breakdown of

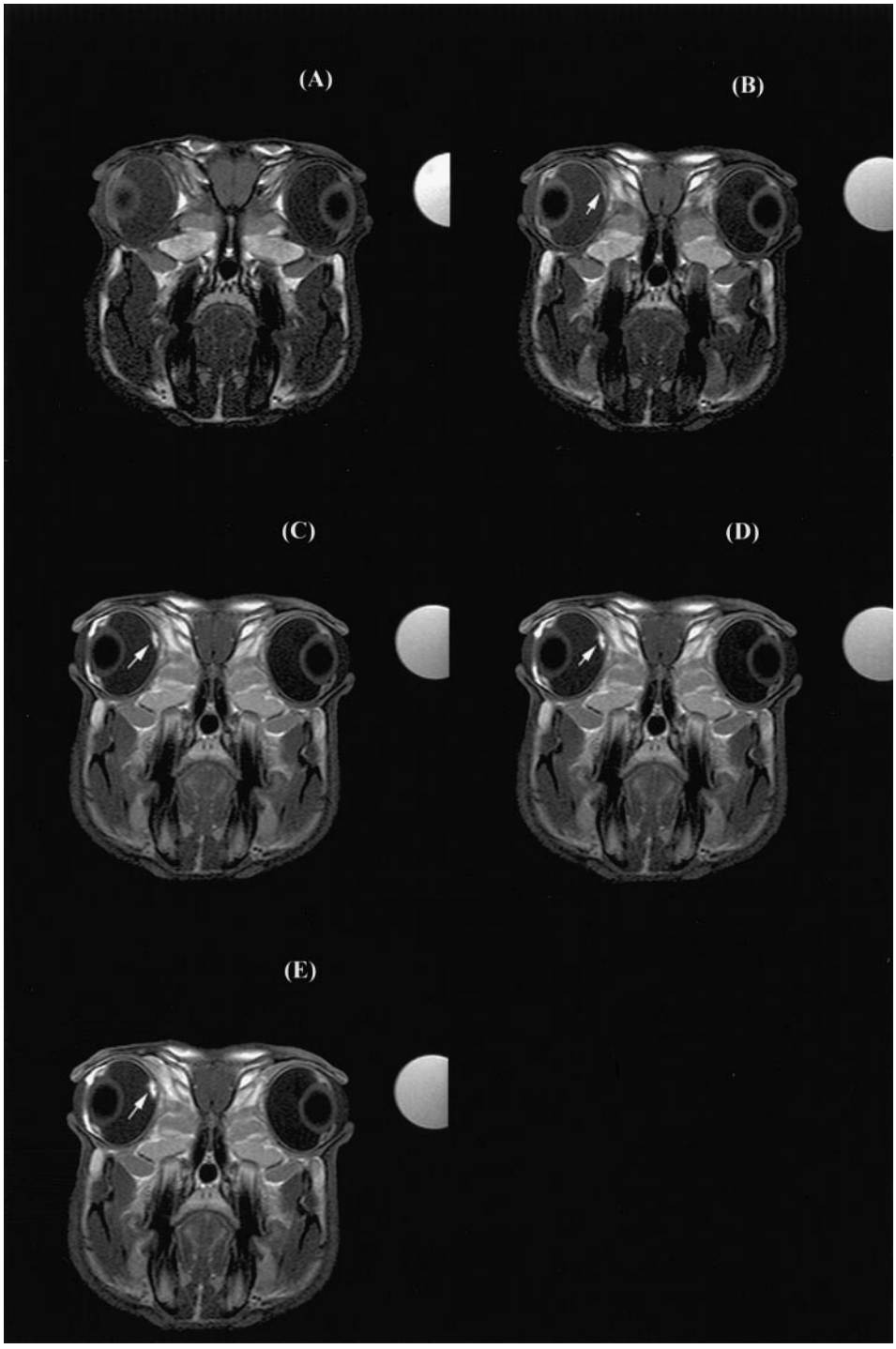

FIGURE 2. These T_1-weighted MR images were acquired 3 days after implantation. They are representative of the MR images that were obtained through the geometric center of both eye globes of the rabbits. (**A**) MR image acquired before injecting the contrast agent AngioMARK. (**B** through **E**) The same MR images as in (**A**), acquired 2, 7, 12, and 16 minutes after injecting AngioMARK, respectively. The *arrow* shows the entry of the contrast agent into the vitreous space of the left eye as indicated by the progressive intensity change. This indicates breakdown of the BRB occurring in the left eye at 3 days after implantation. Note that the control eye remained unchanged throughout this examination.

the BRB of the eye that was implanted with the VEGF-loaded implants was found in four of five animals.

To better interpret the MRI results, clinical fundus photographs and fluorescein angiograms were performed on the eyes of the same set of rabbits. Figure 3A shows the fundus photograph of the control eye of the rabbit of Figure 2, whereas Figure 3B shows the eye with the VEGF implant. These particular images were acquired the day after MR imaging, 4 days after implantation. Figure 3B shows a significant level of retinal vascular dilation and tortuosity. At this implantation time point, Figure 3B shows no presence of newly developed vessels. The control eyes remained normal for all animals. All these findings also were found in the same four of five rabbits.

Figures 4A through 4D are MR images of the same rabbit as in Figure 2 and were acquired 3, 12, 19, and 27 days after implantation, respectively. These are images of the 4th scan after injection of the contrast agent. At 12 days after implantation, of the four animals with the BRB breakdown, only two were still displaying a retinal leakage into the vitreous cavity.

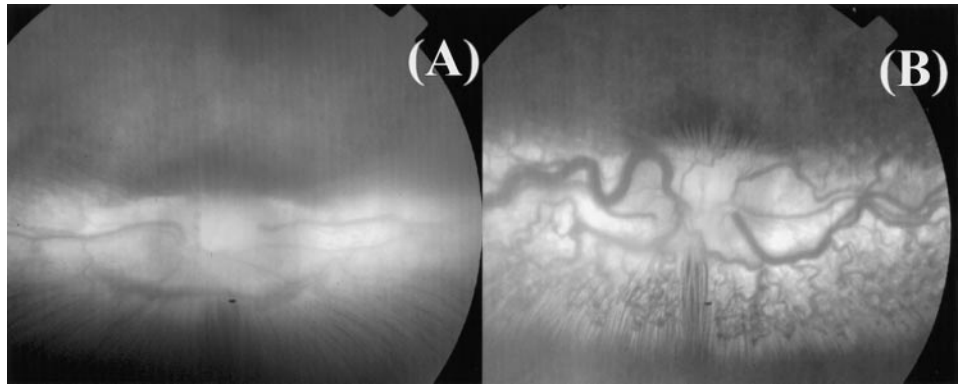

FIGURE 3. Fundus photographs of the same eyes as in Figure 2 taken at 4 days after implantation. (**A**) Representative fundus photograph of the control eye. Note that this control eye remained normal in the presence of the control implant. (**B**) The eye with the VEGF implant. Note the significant level of retinal vascular dilation and tortuosity.

The intensity of this BRB breakdown, as indicated by the intensity change on the T_1-weighted images of the left eye of Figure 4B, is less than at 3 days (Fig. 4A). However, the MR intensity enhancement of the T_1-weighted MR images of the other two animals regressed to below the MRI detection threshold. At 19 days after implantation, a localized retinal detachment was detected in all four animals (Fig. 4C). By 27 days after implantation, a much more advanced retinal detachment is observed on the MR images (Fig. 4D). Because VEGF is a very potent inducer of angiogenesis, we used FA techniques to particularly monitor the presence of newly developed vessels. The presence of these vessels was observed by 18 days after implantation in the eyes that were implanted with the VEGF-loaded devices. The control eyes remained unchanged and normal by all assays during the entire course of this study.

CE-MRI Quantitative Analysis

MR contrast agents, such as Gadolinium-DTPA, have been widely used to investigate abnormal leakage in the blood–brain barrier[15,16] and retinal lesions.[17,18] The alterations in the leakage are used to determine the history of the diseases. A quantitative measure of the leakage can be obtained from the contrast enhanced MR signal intensities using the model of Berkowitz et al.[18] and of Tofts et al.[19] in the case of early

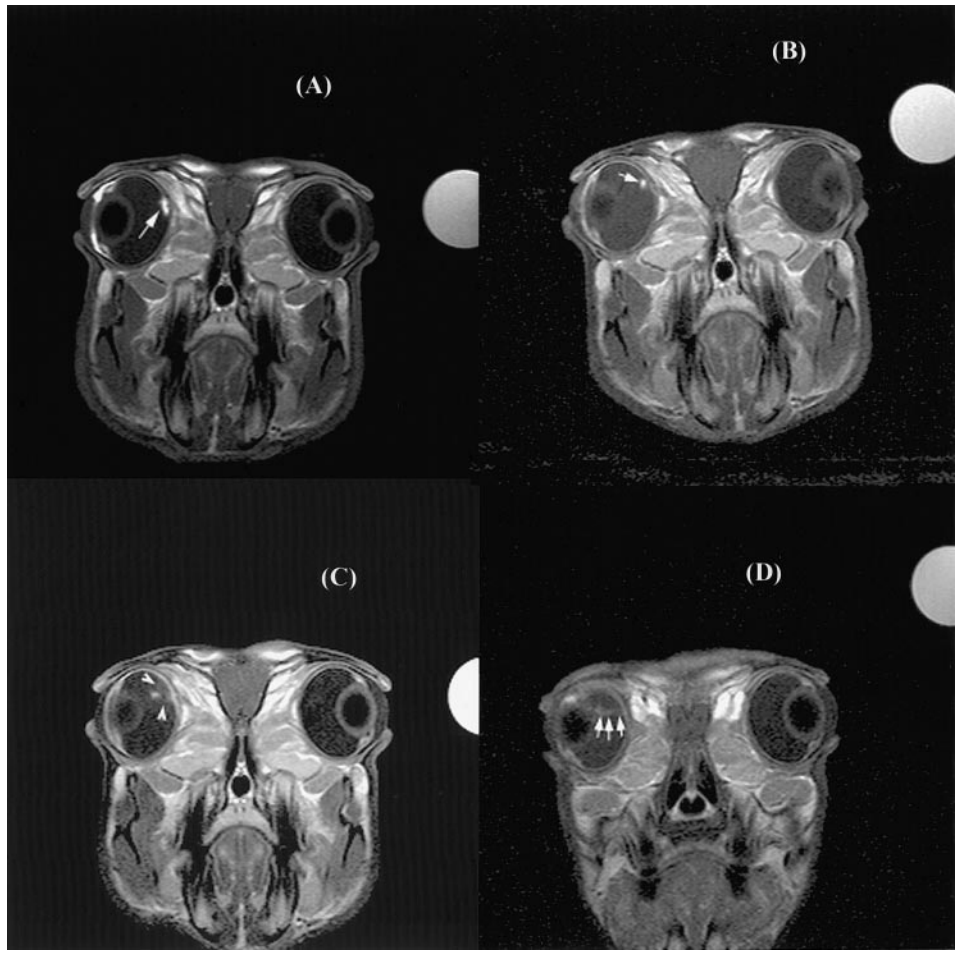

FIGURE 4. These are the MR images of the 4th scan (16 minutes after injection) of the same rabbit eyes as in Figure 2. The images in (**A**) through (**D**) were acquired 3, 12, 19, and 27 days after implantation, respectively. In (**A**) and (**B**) the *arrow* shows the entry of the contrast agent into the vitreous space of the left eye. Note the level of the intensity change as well as of the area of leakage in (**B**), which are less than at 3 days after implantation (**A**), indicating a regression in the retinal leakage by 12 days after implantation. The *arrows* in (**C**) and (**D**) show the progress of the localized retinal detachment. This detachment seems to have started at the same site where the BRB breakdown occurred. Note that the control eye remained unchanged and normal in all animals during the entire course of this study.

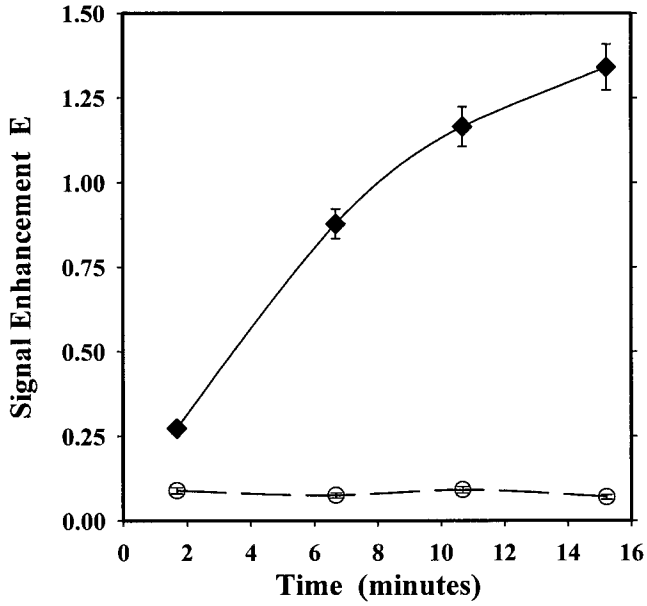

FIGURE 5. This is a representative time course of the enhancement factor *E* after a bolus injection of 0.1 mmol/kg of AngioMARK that was obtained by analyzing the MR images of Figure 2 using Equation 1. (♦), VEGF-implanted eyes; (○), control eyes.

enhancement limit (a brief review is presented in the Appendix). The fractional enhancement (*E*) in the MR signal intensity in the presence of AngioMARK is defined as

$$E = \frac{S(t) - S_0}{S_0} \qquad (1)$$

where $S(t)$ is the spin-echo signal intensity of the ROI within the vitreous that contains all visible enhancement on the final image. In the present study, the final image corresponds to the one obtained on the 4th postinjection images. S_0 is the MR signal intensity of the same ROI before the MR tracer injection. Figure 5 is a representative of the time course of *E* that was obtained by analyzing MR images of Figure 2 using Equation 1. The results show a significant signal enhancement *E* of the VEGF-implanted eyes throughout the 16-minute scan time. However, *E* of control eyes remained unchanged.

Because the present study was performed with the MR contrast agent AngioMARK, to quantify the PS product, the plasma parameters of this tracer must be determined. After IV injection of a bolus dose *D* (mmol/kg body weight) of a tracer given at time $t = 0$, the plasma concentration of this tracer decays exponentially[25]:

$$C_p = D \sum_{i=1}^{2} a_i e^{-m_i t} \qquad (2)$$

where a_i and m_i are the tracer plasma parameters; $i = 1$ describes the early mixing phase between plasma and extracellular water, and $i = 2$ describes the later renal excretion phase. To obtain these parameters, we fitted the data of the plasma concentration decay of AngioMARK in rabbits that was reported by Parmelee et al.[21] to Equation 2 using nonlinear least-squares fit algorithms. These parameters are listed in Table 1.

Using the AngioMARK plasma parameters of Table 1 and the enhancement *E* values (Fig. 5) of each animal eye, we computed the values of PS product as well as of the permeability constant, *k*, of AngioMark from plasma to the vitreous body as described previously[18,19,26] (see also Appendix). This computation was performed on both control and VEGF-implanted eyes at 3 and 12 days after implantation. The values of PS product and *k* constant at $t = 2$, 6.7, 10.7, and 15.2 minutes after injection were averaged together to provide us with a mean PS product and *k* constant values per animal. The mean values of these parameters are summarized in Table 2. Because of retinal detachment (Figs. 4C, 4D), the computation of PS and *k* parameters from the MR images were not possible 12 days after implantation.

DISCUSSION

In this study, we used contrast-enhanced MR imaging to investigate the effects of intravitreal sustained release of VEGF on retinal hyperpermeability in rabbits. The signal intensity enhancement in the T_1-weighted MR images is mainly caused by the T_1 relaxation effect of local contrast agent concentration. This allowed good correlation between the relative signal intensity and local AngioMARK concentration. The use of AngioMARK allowed us to obtain a mean enhancement factor E_m of 1.13 ± 0.13 (mean ± SE); the mean value of *E* of Figure 4 at $t =$ 6.7, 10.7, and 15.2 minutes. This is at least 60% greater than the one obtained when using Gd-DTPA–based contrast agent at a dosage of 1 mmol/kg.[18] Such a gain in enhancement with AngioMARK helped us to define a much better ROI during the drawing of the leaky area, and therefore it provides a more accurate measure of both the PS product and the permeability constant *k*. Furthermore, this gain in enhancement provided a higher sensitivity in detecting the earliest sign of retinal leakage into the vitreous cavity. This enhancement is obtained with AngioMARK dosage of only 0.1 mmol/kg. Such a signal enhancement using this low dosage is extremely desirable in clinical settings. Indeed, this would allow the detection of retinal hyperpermeability in ischemic retinopathies in humans, such as DR, with greater sensitivity using routine clinical doses.

We analyzed the CE-MR images of Figure 2 to quantitate the entry of the AngioMARK into the vitreous, which indicates the breakdown of the BRB This was observed as early as 3 days after implantation. Because control eyes remained unchanged and normal throughout this study, it suggests that this BRB breakdown is mediated solely by the sustained elevation of VEGF in the vitreous. Based on the VEGF in vitro release study, this 3-day BRB breakdown corresponded to the total sustained release of 7.42 ± 0.54 μg/ml of VEGF. We speculate that VEGF promoted retinal vascular leakage by increasing the permeabil-

TABLE 1. AngioMARK Plasma Parameters

Dose *D*	0.1 mmol/kg
m_1	0.198 min^{-1}
a_1	5.5 kg BW/1
m_2	0.0056 min^{-1}
a_2	7.1 kg BW/1

TABLE 2 Permeability Constant, *k,* and PS Product

		VEGF-Implanted Eyes	
	Control Eyes (n = 5)	**3 Days After Implantation (n = 4)**	**12 Days After Implantation (n = 2)**
k (min^{-1})	$4.38 \pm 0.31 \times 10^{-5}$	$8.92 \pm 1.31 \times 10^{-4}$	$4.31 \pm 0.19 \times 10^{-4}$
PS (cm^3/min)	$5.57 \pm 0.66 \times 10^{-7}$	$1.25 \pm 0.25 \times 10^{-5}$	$5.83 \pm 1.38 \times 10^{-6}$

Values are means ± SE. The k and PS values of control eyes remained unchanged throughout this study.

ity of the interendothelial cell tight junctions and inducing vesicular transport across the retinal vascular endothelial cells.[27] Because of the significant level of retinal vascular dilation and tortuosity of the VEGF-implanted eye (Fig. 3B) at 4 days after implantation, increased blood flow is another potential mechanism that might have contributed to induce the BRB breakdown. However, the fact that this BRB breakdown is a consequence of the sustained release of VEGF in the vitreous cavity and that it regressed with time suggests that increased blood flow has little or no role in this BRB breakdown. These results are the most direct evidence that sustained elevation of VEGF in the vitreous cavity is sufficient to cause breakdown of the BRB.

Using the MR image analysis methods as described previously[18,19] (see appendix), we computed the breakdown of the BRB at 3 and 12 days after implantation: PS = $1.25 \pm 0.25 \times 10^{-5}$ and $5.83 \pm 1.38 \times 10^{-6}$ cm^3/min respectively. The control eyes of each animal remained unchanged throughout this study: PS = $5.57 \pm 0.66 \times 10^{-7}$ cm^3/min. The error introduced by approximating the increase of the enhancement E of Figure 5 to a linear function (early enhancement limit) is found to be no more than 15%. This 15% is well within the SE of the calculated mean PS values, which typically range between 20% and 25%. The PS products that we measured show that the BRB breakdown regressed almost by half at 12 days after implantation in two animals and below the MRI detection threshold in the other two animals. In this study, we adopted a 20% E enhancement as our MRI detection threshold. Furthermore, the high value of PS product at 3 days after implantation is strong evidence that the BRB breakdown occurred earlier than 3 days after implantation. Based on the VEGF in vitro study, a total sustained release of 7.42 ± 0.54 μg/ml VEGF in the vitreous cavity is enough to trigger the mechanisms leading to BRB breakdown even earlier than 3 days after implantation of the PLGA-based VEGF release device. The presence of newly developed vessels was observed only at the end of the second week after implantation. This is in agreement with the results that were reported by Ozaki et al.[14] By this time, our VEGF in vitro release study shows that a total of 10.70 ± 0.92 μg/ml of VEGF was released in a sustained fashion. This VEGF amount corresponds approximately to 70% of the total amount of VEGF loaded in the plug.

In a recent study on alloxan-induced diabetic rabbits, Vinores et al[24] reported that 1 year after the induction of diabetes, 5 of 12 eyes examined showed retinal vascular leakage with a mean permeability surface area product PS of 1.73×10^{-5} cm^3/min, and 2 of 6 eyes examined 1.5 years after diabetes induction showed leakage with a mean PS product of 8.66×10^{-6} cm^3/min. The values of our PS product at 3 and 12 days after implantation (PS = $1.25 \pm 0.25 \times 10^{-5}$ and $5.83 \pm 1.38 \times 10^{-6}$ cm^3/min, respectively) are comparable to those obtained from these alloxan-induced diabetic rabbits. This result illustrates the efficacy of sustained elevation of VEGF in the vitreous cavity in causing the breakdown of the BRB.

As shown in Figures 4C and 4D, a retinal detachment also was observed during this same time period. This retinal detachment is probably caused by the vitreous traction that is induced by the newly developed retinal vessels. The progressive retinal complications observed in this study are similar to proliferative DR . Consequently, sustained elevation of VEGF in the vitreous of rabbit eyes could be used as a model for evaluation of pharmacological anti-angiogenic agents to treat or prevent retinal NV and BRB breakdown such as in proliferative DR. This is of considerable importance to humans, because of the growing evidence of the role of VEGF as a major factor in ischemic retinopathies such as DR.[28–30] The noninvasive CE-MRI methods that we used in this study are ideal to assess the quantifiable changes of BRB breakdown in response to the therapeutic intervention in vivo.

In summary, we demonstrate that a total sustained release of 7.42 ± 0.54 μg/ml of VEGF in the vitreous cavity of the rabbit eye is sufficient to cause BRB breakdown even earlier than 3 days after implantation. This retinal permeability regressed by at least a factor of two between 3 and 12 days after implantation. The retinal NV, on the other hand, developed between 12 and 18 days after implantation. After this retinal NV, a retinal detachment occurred. These results are similar to proliferative DR. VEGF antagonists can therefore be tested on this rabbit model to treat or prevent proliferative DR. The in vivo and quantitative CE-MRI method is ideal for these tests.

Acknowledgments

The authors thank Michael Lam and Sidney Gicheru for performing surgery for this study and Epix Medical Inc. for providing the contrast agent AngioMARK.

References

1. Sone H, Kawakami Y, Okuda Y, et al. Ocular vascular endothelial growth factor levels in diabetic rats are elevated before observable retinal proliferative changes. *Diabetologia.* 1997;40:726–730.
2. Ferrara N, Houck K, Jakeman L, Leung DW. Molecular and biological properties of the vascular endothelial growth factor family of proteins. *Endocr Rev.* 1992;13:18–32.
3. Senger DR, Van de Water L, Brown LF, et al. Vascular permeability factor (VPF, VEGF) in tumor biology. *Cancer Metastasis Rev.* 1993;12:3033–3024.
4. Aiello LP, Avery RL, Arrigg PG, et al. Vascular endothelial growth factor in ocular fluid of patients with DR and other retinal disorders [see comments]. *N Engl J Med.* 1994;331:1480–1487.
5. Hammes HP, Lin J, Bretzel RG, et al. Upregulation of the vascular endothelial growth factor/vascular endothelial growth factor receptor system in experimental background diabetic retinopathy of the rat. *Diabetes.* 1998;47:40140–146.

6. Pierce EA, Avery RL, Foley ED, et al. Vascular endothelial growth factor/vascular permeability factor expression in a mouse model of retinal neovascularization. *Proc Natl Acad Sci USA.* 1995;92:905–909.
7. Clermont AC, Aiello LP, Mori F, et al. Vascular endothelial growth factor and severity of nonproliferative diabetic retinopathy mediate retinal hemodynamics in vivo: a potential role for vascular endothelial growth factor in the progression of nonproliferative diabetic retinopathy [see comments]. *Am J Ophthalmol.* 1997; 124:433–446.
8. Gerhardinger C, Brown LF, Roy S, et al. Expression of vascular endothelial growth factor in the human retina and in nonproliferative diabetic retinopathy. *Am J Pathol.* 1998;152:1453–1462.
9. Miyamoto K, Ogura Y, Nishiwaki H, et al. Evaluation of retinal microcirculatory alterations in the Goto–Kakizaki rat. A spontaneous model of non-insulin-dependent diabetes. *Invest Ophthalmol Vis Sci.* 1996;37:898–905.
10. Guerrin M, Moukadiri H, Chollet P, et al. Vasculotropin/vascular endothelial growth factor is an autocrine growth factor for human retinal pigment epithelial cells cultured in vitro. *J Cell Physiol.* 1995;164:385–394.
11. Aiello LP, Northrup JM, Keyt BA, et al. Hypoxic regulation of vascular endothelial growth factor in retinal cells. *Arch Ophthalmol.* 1995;113:1538–1544.
12. Murata T, Nagai R, Ishibashi T, et al. The relationship between accumulation of advanced glycation end products and expression of vascular endothelial growth factor in human diabetic retinas. *Diabetologia.* 1997;40:764–769.
13. Thieme H, Aiello LP, Takagi H, et al. Comparative analysis of vascular endothelial growth factor receptors on retinal and aortic vascular endothelial cells. *Diabetes.* 1995;44:98–103.
14. Ozaki H, Hayashi H, Vinores SA, et al. Intravitreal sustained release of VEGF causes retinal neovascularization in rabbits and breakdown of the blood-retinal barrier in rabbits and primates. *Exp Eye Res.* 1997;64:505–517.
15. Gadian DG, Payne JA, Bryant DJ, et al. Gadolinium-DTPA as a contrast agent in MR imaging—theoretical projections and practical observations. *J Comput Assist Tomogr.* 1985;9:242–251.
16. Sze G. New applications of MR contrast agents in neuroradiology. *Neuroradiology.* 1990;32:421–438.
17. Berkowitz BA, Sato Y, Wilson CA, de Juan E. Blood-retinal barrier breakdown investigated by real-time magnetic resonance imaging after gadolinium-diethylenetriaminepentaacetic acid injection. *Invest Ophthalmol Vis Sci.* 1991;32:2854–2860.
18. Berkowitz BA, Tofts PS, Sen HA, et al. Accurate and precise measurement of blood-retinal barrier breakdown using dynamic Gd-DTPA MRI. *Invest Ophthalmol Vis Sci.* 1992;33:3500–3506.
19. Tofts PS, Berkowitz BA. Measurement of capillary permeability from the Gd enhancement curve: a comparison of bolus and constant infusion injection methods. *Magn Reson Imaging.* 1994; 12:81–91.
20. Lauffer RB, Parmelee DJ, Dunham SU, et al. MS-325: albumin-targeted contrast agent for MR angiography. *Radiology.* 1998;207: 529–538.
21. Parmelee DJ, Walovitch RC, Ouellet HS, Lauffer RB. Preclinical evaluation of the pharmacokinetics, biodistribution, and elimination of MS-325, a blood pool agent for magnetic resonance imaging. *Invest Radiol.* 1997;32:741–747.
22. Wilson CA, Fleckenstein JL, Berkowitz BA, Green ME. Preretinal neovascularization in diabetic retinopathy: a preliminary investigation using contrast-enhanced magnetic resonance imaging. *J Diabetes Complications.* 1992;6:223–229.
23. Wood GK, Berkowitz BA, Wilson CA. Visualization of subtle contrast-related intensity changes using temporal correlation. *Magn Reson Imaging.* 1994;12:101310–101320.
24. Vinores SA, Derevjanik NL, Mahlow J, et al. Electron microscopic evidence of the mechanics of blood-retinal barrier breakdown in diabetic rabbits: comparison with magnetic resonance imaging. *Pathol Res Pract.* 1998;194:497–505.
25. Tofts PS, Kermode AG. Measurement of the blood-brain barrier permeability and leakage space using dynamic MR imaging. 1. Fundamental concepts. *Magn Reson Med.* 1991;17:357–367.
26. Wilson CA, Berkowitz BA, Funatsu H, et al. Blood-retinal barrier breakdown following experimental retinal ischemia and reperfusion. *Exp Eye Res.* 1995;61:547–557.
27. Luna JD, Chan CC, Derevjanik NL, et al. Blood-retinal barrier (BRB) breakdown in experimental autoimmune uveoretinitis: comparison with vascular endothelial growth factor, tumor necrosis factor alpha, and interleukin-1beta-mediated breakdown. *J Neurosci Res.* 1997;49:268–280.
28. Boulton M, Foreman D, Williams G, McLeod D. VEGF localisation in diabetic retinopathy. *Br J Ophthalmol.* 1998;82:561–568.
29. Mathews MK, Merges C, McLeod DS, Lutty GA. Vascular endothelial growth factor and vascular permeability changes in human diabetic retinopathy. *Invest Ophthalmol Vis Sci.* 1997;38:2729–2741.
30. Vinores SA, Youssri AI, Luna JD, et al. Upregulation of vascular endothelial growth factor in ischemic and non-ischemic human and experimental retinal disease. *Histol Histopathol.* 1997;12:99–109.
31. Tofts PS, Kermode AG. Measurements of blood-brain barrier permeability and leakage space using dynamic MR imaging. *Magn Reson Med.* 1991;17:357–367.
32. Yang L, Fassihi R. Zero-order release kinetics from a self-correcting floatable asymmetric configuration drug delivery system. *J Pharm Sci.* 1996;85:170–173.

APPENDIX

After IV injection of a bolus dose D (mmol/kg body weight) of a tracer, such as AngioMARK, given at time $t = 0$, the plasma concentration of this tracer decays exponentially[25]:

$$C_p = D \sum_{i=1}^{2} a_i e^{-m_i t} \qquad (A1)$$

where a_i and m_i are the tracer plasma parameters; $i = 1$ describes the early mixing phase between plasma and extracellular water, and $i = 2$ describes the later renal excretion phase. To obtain these parameters, the measured decay plasma concentration of the tracer could be fit to Equation 1 using a nonlinear least-squares algorithm. This technique was used to fit the data that was reported by Parmelee et al.[21] to obtain the AngioMARK plasma parameters. These AngioMARK plasma parameters are listed in Table 1.

The resulting tissue or vitreous concentration is[18,25]

$$C_v = D\,k \sum_{i=1}^{2} a_i(1 - e^{-m_i t})/m_i \qquad (A2)$$

where k is the transfer constant or permeability.

The MRI signal from a spin-echo pulse sequence with short TEs is given by:

$$S(t) = \rho(1 - e^{-TR/T_1}) \qquad (A3)$$

where ρ is the spin density, TR is the repetition time, and T_1 is the longitudinal MR relaxation time in the presence of AngioMARK. The relaxation rate, $1/T_1$, is expressed as

$$\frac{1}{T_1} = \frac{1}{T_{10}} + R_1 C_t \qquad (A4)$$

where R_1 is the relaxivity of AngioMARK, $R_1 = 32.5 \pm 2.3$ l/mmol/kg in rabbit plasma,[20] and T_{10} is T_1 in the absence of the tracer ($T_{10} = 4$ seconds).

The calculation of the parameter k is from the MR signal enhancement E, which is defined as the fractional increase in signal in the presence of AngioMARK:

$$E = \frac{S(t) - S_0}{S_0} \tag{A5}$$

where S_0 is the MR signal intensity before the tracer injection.

In the early enhancement limit, E can be approximated to a linear function[19]:

$$E = R_1 T_k C_v \tag{A6}$$

where

$$T_k = TR \frac{e^{-TR/T_{10}}}{1 - e^{-TR/T_{10}}} \tag{A7}$$

By substituting Equation A2 into A6, we obtain the relationship linking k to E:

$$k = \frac{E}{R_1 T_k D \sum_{i=1}^{2} a_i (1 - e^{-m_i t})/m_i} \tag{A8}$$

Therefore, the permeability k can be obtained from a single enhancement value at a particular time t after AngioMARK IV injection.

The permeability surface area, PS, product (cm^3/min) for a lesion where leakage is contained within the slice thickness (St) is[18,19,31]

$$PS = k\, A_{ROI}\, St \tag{A9}$$

where A_{ROI} is the area of the region of interest used to measure the enhancement.